ARMY RESEARCH LABORATORY

# Molecular Simulation of Shocked Materials Using Reaction Ensemble Monte Carlo: Part I. Application to Nitrogen Dissociation

**by John K. Brennan and Betsy M. Rice**

**ARL-TR-3983** **November 2006**

## NOTICES

### Disclaimers

The findings in this report are not to be construed as an official Department of the Army position unless so designated by other authorized documents.

Citation of manufacturer's or trade names does not constitute an official endorsement or approval of the use thereof.

Destroy this report when it is no longer needed. Do not return it to the originator.

**Army Research Laboratory**
Aberdeen Proving Ground, MD 21005-5066

**ARL-TR-3983** **November 2006**

# Molecular Simulation of Shocked Materials Using Reaction Ensemble Monte Carlo: Part I. Application to Nitrogen Dissociation

**John K. Brennan and Betsy M. Rice**
**Weapons and Materials Research Directorate, ARL**

| REPORT DOCUMENTATION PAGE | Form Approved OMB No. 0704-0188 |
|---|---|



| 1. REPORT DATE *(DD-MM-YYYY)* | 2. REPORT TYPE | 3. DATES COVERED (From - To) |
|---|---|---|
| November 2006 | Final | January 2005–May 2005 |

**4. TITLE AND SUBTITLE**
Molecular Simulation of Shocked Materials Using Reaction Ensemble Monte Carlo: Part I. Application to Nitrogen Dissociation

**5a. CONTRACT NUMBER**

**5b. GRANT NUMBER**

**5c. PROGRAM ELEMENT NUMBER**

**6. AUTHOR(S)**
John K. Brennan and Betsy M. Rice

**5d. PROJECT NUMBER**
H4311

**5e. TASK NUMBER**

**5f. WORK UNIT NUMBER**

**7. PERFORMING ORGANIZATION NAME(S) AND ADDRESS(ES)**
U.S. Army Research Laboratory
ATTN: AMSRD-ARL-WM-BD
Aberdeen Proving Ground, MD 21005-5066

**8. PERFORMING ORGANIZATION REPORT NUMBER**
ARL-TR-3983

**9. SPONSORING/MONITORING AGENCY NAME(S) AND ADDRESS(ES)**

**10. SPONSOR/MONITOR'S ACRONYM(S)**

**11. SPONSOR/MONITOR'S REPORT NUMBER(S)**

**12. DISTRIBUTION/AVAILABILITY STATEMENT**
Approved for public release; distribution is unlimited.

**13. SUPPLEMENTARY NOTES**

**14. ABSTRACT**
We demonstrate the applicability of the Reaction Ensemble Monte Carlo (RxMC) simulation method for calculating the shock Hugoniot properties of a material. The method does not require interaction potentials that simulate bond breaking or bond forming; it requires only the intermolecular potentials and the ideal-gas partition functions for the reactive species that are present. By performing Monte Carlo sampling of forward and reverse reaction steps, RxMC provides information on the chemical equilibria states of the shocked material including the density of the reactive mixture and the mole fractions of the reactive species. We illustrate the methodology for shocked liquid $N_2$, where we find excellent agreement with experimental measurements. This is the first of two reports describing the applicability of the RxMC method to simulating the shock Hugoniot properties of materials.

**15. SUBJECT TERMS**
molecular simulation, Monte Carlo, Hugoniot, reaction ensemble

| 16. SECURITY CLASSIFICATION OF: | | | 17. LIMITATION OF ABSTRACT | 18. NUMBER OF PAGES | 19a. NAME OF RESPONSIBLE PERSON |
|---|---|---|---|---|---|
| a. REPORT | b. ABSTRACT | c. THIS PAGE | | | John K. Brennan |
| UNCLASSIFIED | UNCLASSIFIED | UNCLASSIFIED | UL | 32 | 19b. TELEPHONE NUMBER (*Include area code*) 410-306-0678 |

**Standard Form 298 (Rev. 8/98)**
**Prescribed by ANSI Std. Z39.18**

## Contents

## List of Figures



## List of Tables

## Acknowledgments

The authors wish to thank Martin Lisal (Institute of Chemical Process Fundamentals, Academy of Sciences of the Czech Republic) for helpful discussions and critical reading of this manuscript. This work was performed while John K. Brennan held a National Research Council Research Associateship Award at the U.S. Army Research Laboratory. The calculations reported in this work were performed at the U.S. Army Research Laboratory Major Shared Resource Center, Aberdeen Proving Ground, MD.

INTENTIONALLY LEFT BLANK.

# 1. Introduction

The behavior of materials under conditions of extreme temperature and pressure is of critical importance in many fields of physics and fluid science (*1–3*). The properties of materials at these conditions can be measured through shock experiments, which are capable of producing pressures up to several hundred GPa and temperatures exceeding 10,000 K. Moreover, determining the shock properties of energetic materials is a crucial task in the field of detonation science (*4*).

Experimental measurements of the properties of shocked materials are often difficult because instrumentation must be capable of spanning a wide range of pressures (1–300 GPa) and temperatures (500–15000 K). Additionally, energy releases that might accompany a material under shock conditions, as well as the time and length scales over which the event occurs, have thwarted extensive experimental studies of many fundamental substances. As a further complication, recent theoretical predictions suggest that the detonation products of some systems supercritical phase separate, significantly altering the shock properties (e.g., references [*5–7*]. Unfortunately, current experimental techniques are not capable of delineating the phase separation of materials under shock conditions; thus, this behavior has yet to be verified.

Such laboratory challenges have necessitated the development of theoretical predictive capabilities to complement the experimental analyses. To date, the most reliable theoretical treatments for predicting shock properties apply statistical mechanical approaches such as variational perturbation theory (e.g., Ross [*8*] or integral equation theory (e.g., references [*9–11*]). These approaches predict the shock properties by minimizing the Gibbs free-energy and by requiring that the total number of elements constituting the chemically reacting species is conserved. Thermochemical software such as the chemical equilibrium code (*12*) and Cheetah (*13*) are capable of performing such calculations. However, these approaches require accurate equations of state (EOS) for the reactive mixture, thus limiting the prediction of the shock properties of materials to those for which equations of state are available. The calculations also require heats of formation and densities of the unshocked material. These quantities are often unknown for notional or novel energetic materials as well as for materials in highly nonideal environments (e.g., energetic materials packed in polymer matrices or confined in carbon nanotubes). Furthermore, approximations must often be made within the theoretical models to keep the calculations tractable, for example, to develop an analytical representation of the fluid equation of state (*11*) or in applying the van der Waals one-fluid approximation (*12*, *13*). These types of approximations can add uncertainty to the predictive capabilities of the methods.

A powerful simulation method available for studying the shock properties of materials while providing insight into atomic-level phenomena is the molecular dynamics (MD) method (*14–31*). The method can be used irrespective of rate limitations, the production of huge energy releases,

extreme thermodynamic conditions, or other regimes that are presently inaccessible by experimental methods. MD evaluation of the Hugoniot states of a material can be accomplished by calculating properties behind the shock discontinuity in a shockwave simulation (*30*) or by generating an EOS for subsequent evaluation of the Hugoniot conservation relations (*24*, *27*). Recently, an equilibrium MD method has been introduced, termed uniaxial Hugoniostat (*29*), which utilizes equations of motion that constrain the system during the MD simulation such that the time-averaged properties correspond to those on the shock Hugoniot curve. For evaluating the shock Hugoniot of a material, the uniaxial Hugoniostat technique is more efficient than the method of generating an EOS using standard MD for subsequent evaluation of the conservation equations (*24*, *27*). A significant drawback of all MD approaches, however, is that they require an accurate model of the interaction potential experienced between all species in the shocked and unshocked states. If the relative species concentrations of the products in the shocked state of interest are not known, then the MD approach requires an interaction potential that simulates bond breaking and bond formation in order to establish the chemical equilibrium of the final shocked state. Although significant advances have been made in developing potentials that reproduce the characteristics of a detonation, the potentials are still highly idealized representations of the energetic molecular system (*14–23*, *25–28*). However, if the relative species concentrations are known at the conditions of the shocked state, then generating the shock Hugoniot curve using either the conventional or the uniaxial Hugoniostat MD method only requires appropriate potentials that describe nonreacting interactions among all species present.

One of several alternative methods for calculating chemically reactive systems which is appropriate for determining the shock properties of materials is Reaction Ensemble Monte Carlo (RxMC) (*32*, *33*). RxMC circumvents some of the problems associated with conventional and uniaxial Hugoniostat MD methods. RxMC requires neither a priori knowledge of the relative concentrations of the species in the shocked state nor a potential that describes bond breaking or bond formation. The method only requires (a) functions that accurately describe nonreactive interactions between all possible species in the equilibrium mixture of the final shocked state (i.e., intermolecular potentials) and (b) ideal gas partition functions for all species in the mixture. For a given intermolecular potential model, the method will provide information on the chemical equilibrium state, such as the density of the reactive mixture, the mole fractions of reactive species, the change in the total number of moles, and the internal energy. The intermolecular model can contain various levels of detail including multisite molecules and electrostatic contributions. Numerous reactions can be simulated simultaneously in multiple phase systems by performing Monte Carlo sampling of forward and reverse reaction steps. Using the RxMC method, the dependence of the chemical equilibria on system conditions such as temperature, pressure, and the surrounding environment (e.g., a condensed phase or highly nonideal environment) can be studied.

In this work, we demonstrate the applicability of RxMC for calculating the shock Hugoniot properties of materials. We illustrate the method on shocked liquid $N_2$, which dissociates into atomic nitrogen (N) within a particular thermodynamic regime. This reaction has been studied extensively by both experimental and theoretical techniques. This report is the first of two reports that illustrate the RxMC method. In the second report (*34*), we consider shocked liquid NO, which is (nearly) an irreversible decomposition reaction that generates a mixture of homonuclear products ($N_2$ and $O_2$).

The outline of the report is as follows. The RxMC methodology applied to the simulation of the shock properties of materials is described in section 2. Simulation details and models can be found in section 3 and application of the method to shocked liquid $N_2$ is presented in section 4.

## 2. Methodology

### 2.1 Reaction Ensemble Monte Carlo

The RxMC method (32, 33) is designed to minimize the Gibbs free-energy, thus determining the true chemical equilibrium state irrespective of rate limitations. RxMC requires intermolecular potentials for the molecular species that are present in the reactive mixture and often uses spherically-averaged potentials such as Lennard-Jones or Exponential-6 models (35). RxMC also requires inputting the ideal-gas internal modes (vibration, rotation, and electronic) for each reactive species. These contributions can be included by calculating internal partition functions from molecular energy-level data (32) or by using tabulated thermochemical data (33). Regardless of the approach taken, the required information is readily available in standard sources (35–37) or can be generated using quantum mechanical calculations. Finally, the particular reactions occurring in the system must be specified. Provided that a sufficient set of independent reactions are specified, this requirement is not a considerably limiting factor since insignificant reactions are easily discernable by negligible product concentrations.

RxMC implementation provides information on the chemical equilibrium state, such as the density of the reactive mixture, mole fractions of reactive species, the change in the total number of moles, and the internal energy. RxMC can be performed in many different types of ensembles, including canonical, isothermal-isobaric, Gibbs (*38*), and other less common ensembles (*39*). Furthermore, RxMC can be performed for multiple reactions and multiple phases (*32*, *33*, *38*, *40–46*). RxMC does not simulate bond breaking or forming; these relatively rare events in standard Metropolis Monte Carlo (*47*) would result in considerable statistical uncertainty. Rather, RxMC directly samples forward and reverse reaction steps as Monte Carlo-type moves according to the stoichiometry of the reactions being sampled. The isothermal-

isobaric version of the RxMC method containing $J$ number of reactions involves the following trial moves:

1. a change in the position or orientation of a molecule, chosen at random;
2. a forward step for randomly chosen reaction $j$, in which reactant molecules are chosen at random and changed to product molecules;
3. a reverse step for randomly chosen reaction $j$, in which product molecules are chosen at random and changed to reactant molecules; and
4. a random change in the simulation box volume.

Step 1 ensures that thermal equilibrium is established for the user-specified temperature, steps 2 and 3 ensure that chemical equilibrium is established, while step 4 satisfies the requirement of mechanical equilibrium for the user-specified pressure. Note that the transition probabilities in steps 2 and 3 do not require specifying the values of the chemical potentials nor chemical potential differences for any of the mixture components.

The acceptance probability of state $k$ going to state $l$ for a particle displacement or orientation step is given by

$$P_{kl}^{dis} = \min\{1, \exp(-\beta \Delta U_{kl})\}, \tag{1}$$

where $\Delta U_{kl} = U_l - U_k$ is the change in the configurational energy and $\beta = 1/k_B T$; $k_B$ is the Boltzmann constant and $T$ is the temperature.

The acceptance probability for a reaction step is given by

$$P_{j,kl}^{rxn} = \min\left\{1, \prod_{i=1}^{c_j} \frac{N_i!}{(N_i + \nu_{ji}\xi_j)!} \left(\frac{q_{\text{int},i} V}{\Lambda_i^3}\right)^{\nu_{ji}\xi_j} \exp(-\beta \Delta U_{kl})\right\}, \tag{2}$$

where $c_j$ is the total number of species in reaction $j$; $N_i$ is the total number of molecules of species $i$; $\nu_{ji}$ is the stoichiometric coefficient of species $i$ in reaction $j$; $\xi_j$ is the molecular extent of reaction for reaction $j$; $q_{\text{int},i}$ is the quantum partition function for the internal modes of an isolated molecule of species $i$, which includes vibrational, rotational, and electronic; $\Lambda_i$ is the thermal de Broglie wavelength of species $i$; and $V$ is the total volume of the system. Equation 2 is appropriate for both forward and reverse reaction steps ($\xi_j = 1$ for a forward step and $\xi_j = -1$ for a reverse step), where the stoichiometric coefficients are taken to be positive for product species and negative for reactant species. (For example, consider the reaction A⇔2B. For the reaction as written, the stoichiometric coefficients for species A and B are $\nu_A = -1$ and $\nu_B = +2$ while $\xi = +1$. Then for the reverse reaction step, $\nu_A$ and $\nu_B$ again are –1 and +2, respectively, but now $\xi = -1$.)

Finally, a random change in the simulation box volume is accepted with the probability

$$P_{kl}^{vol} = \min\left\{1, \exp\left( -\beta\Delta U_{kl} - \beta P_{imp}(V_l - V_k) + N \ln\frac{V_l}{V_k} \right)\right\}, \quad (3)$$

where $P_{imp}$ is the user-specified, or imposed, pressure. Derivations of these transition probabilities along with further details of the methodology can be found in the original papers (*32*, *33*, *38*).

## 2.2 Calculation of Shock Hugoniot Properties

The thermodynamic quantities of a material in the initial unshocked state and the final shocked state are related by the conservation equations of mass, momentum, and energy across the shock front as follows (*4*):

$$\text{Mass:} \qquad \rho_o D = \rho(D - u). \quad (4)$$

$$\text{Momentum:} \quad P - P_o = \rho_o u D. \quad (5)$$

$$\text{Energy:} \qquad E - E_o = \tfrac{1}{2}(P + P_o)(V_o - V)\ . \quad (6)$$

In equations 4–6, $E$ is the specific internal energy, $P$ is the pressure, $\rho$ is the specific density, $V = 1/\rho$ is the specific volume, $D$ is the velocity of the shock wave propagating through the material, and $u$ is the mass velocity of the products behind the shock wave. The term "specific" refers to the quantity per unit mass, while the subscript "o" refers to the quantity in the initial unshocked state.

The shock wave velocity $D$ can be calculated by solving equations 4 and 5 for the mass velocity $u$ and equating these expressions. The resulting expression, termed the Rayleigh line, can be written as

$$R = \rho_o^2 D^2 - (P - P_o)(V_o - V) = 0\ . \quad (7)$$

The so-called *Hugoniot* function satisfies equation 6 as

$$H_g(T,V) = 0 = E - E_o - \tfrac{1}{2}(P + P_o)(V_o - V)\ . \quad (8)$$

Note that the quantities $E$ and $V$ are extensive quantities in equations 6–8 and thus dependent on the relative amounts of the reactive species. The extensive quantities used in this work were formulated on a specific basis (per gram); alternatively, these quantities can be formulated on a total system basis (total number of moles). The relative amounts of the reactive species along with the quantities $E$, $P$, and $V$ are calculated explicitly during the RxMC simulation. The internal energy is calculated during the RxMC simulation based upon the following derivation. The thermodynamic definition of the internal energy is given as

$$E \equiv H - PV\ , \quad (9)$$

where $H$ is the specific enthalpy that can be written as a sum of the ideal-gas ($H^{o}$) and excess enthalpies ($H^{e}$):

$$H = H^{o} + H^{e} . \tag{10}$$

The ideal-gas and excess enthalpies can be written as

$$H^{o} = \sum_{i=1}^{c_j} y_i H_i^{o} \tag{11}$$

and

$$H^{e} = U^{conf} + PV - RT , \tag{12}$$

so that

$$H = \sum_{i=1}^{c_j} y_i H_i^{o} + U^{conf} + PV - RT . \tag{13}$$

$U^{conf}$ is the total configurational energy calculated during the simulation from the species-species interactions; $y_i$ is the mole fraction of species $i$; $c_j$ is the total number of species; $H_i^{o}$ is the specific ideal-gas enthalpy of pure species $i$, which can be determined solely from tabulated thermochemical data at the appropriate temperature, $T$ (*37*, *48*, *49*), or with tabulated thermochemical data supplemented with computed values where data is lacking (e.g., [*50, 51*]); and R is the universal gas constant. Substituting equation 13 into equation 9,

$$E = \sum_{i=1}^{c_j} y_i H_i^{o} + U^{conf} - RT , \tag{14}$$

which is the specific internal energy expression needed in equation 8.

The search algorithm for locating a point on the Hugoniot curve used in this study is as follows:

Step 1: For a user-specified pressure, P, a few RxMC-NPT simulations were performed at temperatures believed to be near Hg(T,V) = 0.

Step 2: A functional form for the Hg vs. T plot is determined, e.g., fitted to a quadratic polynomial, and the temperature ($T_{Hg}$) that satisfies equation 8 at Hg = 0 is interpolated.

Step 3: Similarly, functional forms for the other desired quantities (V, E, D) were determined and interpolated at $T_{Hg}$.

Depending on the initial guess of $T_{Hg}$, additional RxMC simulations may be required to achieve the desired accuracy. Typically, 4–6 RxMC simulations are needed to determine a single point on the Hugoniot curve, where best results are obtained when chosen values of $T$ include both $H_g>0$ and $H_g<0$. Steps 1–3 are then repeated to trace out the entire Hugoniot curve.

## 3. Simulation Model and Details

### 3.1 Intermolecular Potential Models

The species particles interact through the exponential-six potential, which can be expressed as:

$$U_{\exp-6}(r) = \begin{cases} \infty & r < r_{\text{core}} \\ \dfrac{\varepsilon}{1-6/\alpha}\left[\dfrac{6}{\alpha}\exp\left(\alpha\left[1-\dfrac{r}{r_m}\right]\right) - \left(\dfrac{r_m}{r}\right)^6\right] & r \geq r_{\text{core}} \end{cases}, \qquad (15)$$

where $\varepsilon$ is the depth of the attractive well between particles, $r_m$ is the radial distance at which the potential is a minimum, while $\alpha$ controls the steepness of the repulsive interaction. The cutoff distance $r_{\text{core}}$ is included to avoid the unphysical singularity in the potential function as r→0. The potential parameters for the species considered in this work are given in table 1. A spherical cutoff of $2.5r_{m,\text{N2}}$ was applied with long range corrections added to account for interactions beyond this distance (*52*). Electrostatic contributions were ignored between species. The unlike interactions between species *i* and *j* were approximated by the Lorentz-Berthelot mixing rules (*35*) for $\varepsilon_{ij}$, $\alpha_{ij}$, and $r_{m,ij}$:

$$\varepsilon_{ij} = (\varepsilon_i\varepsilon_j)^{1/2}\,;\ \alpha_{ij} = (\alpha_i\alpha_j)^{1/2}\,;\ r_{m,ij} = (r_{m,i} + r_{m,j})/2\ ,$$

while

$$r_{\text{core},ij} = (r_{\text{core},i} + r_{\text{core},j})/2\ . \qquad (16)$$

Table 1. Exponential-6 potential parameters.

| Species | $r_{\text{core}}$ (Å) | $r_m$ (Å) | $\varepsilon/k_B$ (K) | $\alpha$ | Source (Reference No.) |
|---|---|---|---|---|---|
| $N_2$ | 1.13 | 4.2005 | 101.10 | 12.684 | (*11*) |
| N | 0.98 | 2.5688 | 88.181 | 11.013 | (*11*) |

The vibrational and rotational contributions to the ideal-gas partition function of $N_2$ used in simulating the $N_2$ dissociation reaction were calculated using a standard source (*36*) and supplemented with electronic level constants that included the ground state and six excited electronic states (*48*). For N, the electronic energy levels were taken from Moore and Gallagher (*49*). The corresponding thermochemical reference data were used in calculating the ideal-gas enthalpies ($H_i^o$) required in equation 11 (*37*, *48*, *49*).

### 3.2 Simulation Details

Constant-pressure RxMC simulations of shocked $N_2$ were initiated from 3375 $N_2$ particles placed on a face-centered-cubic lattice structure. The standard periodic boundary conditions and minimum image convention were used (*53*). Simulations were performed in steps, where a step (chosen with equal probability) was either a particle displacement, forward reaction step, or reverse reaction step. A change in the simulation cell volume was attempted every 2500 steps. Simulations were equilibrated for $0.3 \times 10^7$ steps after which averages of the quantities were taken over $2.0 \times 10^7$ steps. Uncertainties were estimated using the method of block averages by dividing the production run into 10 equal blocks (*52*). Reported uncertainties are one standard deviation of the block averages. The maximum displacement and volume change were adjusted to achieve an acceptance fraction of ~0.33 and 0.5, respectively. Depending on the system conditions, the acceptance fraction of the reaction steps ranged from 0.075–0.375. Calculated quantities were reduced by the exponential-6 potential energy ($\varepsilon$) and size ($r_m$) parameters of $N_2$.

## 4. Application

We consider shocked $N_2$ in the pressure range 3–90 GPa for which reliable experimental data are available (*54*, *55*). At pressures between ~30–100 GPa, the N≡N triple bond is destabilized and molecular nitrogen dissociates into atomic nitrogen (*56*, *57*). At higher pressures, theory suggests that nitrogen can exist as a metastable polymeric phase of N atom clusters that are covalently bonded (*58–62*), before losing this covalency at still higher pressures. In the present work, we consider only the regime where molecular nitrogen is believed to dissociate into atomic nitrogen, $N_2 \Leftrightarrow 2N$. Analogous to the work of Fried and Howard (*11*), we consider two models for this reaction, a reactive model that includes the dissociation reaction, and a nonreactive model that does not.

We determined the shock Hugoniot properties of liquid $N_2$ using the calculated initial states given in table 2. The values given in table 2 were determined by performing a canonical ensemble (constant-N*VT*) Monte Carlo simulation of N = 3375 $N_2$ molecules at $T$ = 77.0 K and at a specific volume of $V$ = 1.238 $cm^3/g$. A comparison of the pressure and internal energy determined from this N*VT* simulation with experiment is given in table 2. The shock Hugoniot properties were determined by carrying out the prescription outlined in section 2.2. The raw data determined from a series of constant-pressure RxMC simulations at several different temperatures are given in table 3. Also reported in table 3 are the values of the Hugoniot expression (equation 8) using the predicted thermodynamic data. Quadratic polynomials were used in the fitting procedure of steps 2 and 3 (see section 2.2) with the exception of the shock wave velocity ($D$), where a linear equation was used. A comparison of the shock properties along the principal Hugoniot calculated from the RxMC simulations and the available

Table 2. Initial fluid state used to evaluate equation 8.

| **Thermodynamic Property** | **Liquid $N_2$** | |
|---|---|---|
| | **Experiment** (*55*) | **N*VT*-MC** |
| Temperature, $T$ (K) | 77.0 ± 0.5 | 77.0 |
| Density, $\rho$ (g/cm$^3$) | 0.808 ± 0.003 | 0.808 |
| Pressure, $P$ (MPa) | — | 50.49 ± 0.02 |
| Energy, $E$ (kJ/g) | — | –0.441 ± 0.004 |

Table 3. Constant-pressure RxMC simulations of shocked liquid $N_2$.

| **T (K)** | **<*P*> (GPa)** | **Mole Fraction[a]** | | **<*V*> (cm$^3$/g)** | **<$U^{conf}$> (kJ/g)** | ***H*$^{ob}$ (kJ/g)** | ***E*$^{c}$ (kJ/g)** | **$H_g$[d] (kJ/g)** | ***D*$^{e}$ (km/s)** |
|---|---|---|---|---|---|---|---|---|---|
| | | **<x($N_2$)>** | **< x(N)>** | | | | | | |
| **$P_{imp}$ = 2.96 GPa** | | | | | | | | | |
| 475 | 3.010(2) | 1.0000 | 0.0000 | 0.7532(8) | 0.182(2) | 0.1852 | 0.227 | –0.0732 | 3.059 |
| 500 | 3.008(1) | 1.0000 | 0.0000 | 0.7572(7) | 0.188(2) | 0.2110 | 0.250 | –0.0429 | 3.071 |
| 525 | 3.008(2) | 1.0000 | 0.0000 | 0.7606(9) | 0.192(3) | 0.2379 | 0.274 | –0.0138 | 3.082 |
| 550 | 3.008(2) | 1.0000 | 0.0000 | 0.7646(9) | 0.197(3) | 0.2643 | 0.298 | 0.0165 | 3.094 |
| **$P_{imp}$ = 4.74 GPa** | | | | | | | | | |
| 850 | 4.795(3) | 1.0000 | 0.0000 | 0.7047(6) | 0.463(4) | 0.5955 | 0.806 | –0.0433 | 3.693 |
| 900 | 4.795(3) | 0.9998(1) | 0.0002(1) | 0.7090(8) | 0.471(3) | 0.6566 | 0.860 | 0.0210 | 3.708 |
| 950 | 4.790(3) | 0.9997(1) | 0.0003(1) | 0.7132(6) | 0.478(5) | 0.7201 | 0.916 | 0.0879 | 3.721 |
| **$P_{imp}$ = 10.0 GPa** | | | | | | | | | |
| 1950 | 10.072(7) | 1.0000 | 0.0000 | 0.6197(9) | 1.249(7) | 1.9407 | 2.611 | –0.0751 | 4.984 |
| 2000 | 10.081(4) | 0.9998(1) | 0.0002(1) | 0.6210(6) | 1.254(9) | 2.0101 | 2.670 | –0.0115 | 4.992 |
| 2050 | 10.066(8) | 0.9998(1) | 0.0002(1) | 0.6235(6) | 1.260(9) | 2.0749 | 2.726 | 0.0609 | 4.998 |
| **$P_{imp}$ = 18.1 GPa** | | | | | | | | | |
| 3850 | 18.195(2) | 0.9997(1) | 0.0003(1) | 0.5549(7) | 2.398(2) | 4.4512 | 5.707 | –0.0806 | 6.380 |
| 3900 | 18.191(2) | 0.9997(1) | 0.0003(1) | 0.5557(7) | 2.401(1) | 4.5179 | 5.761 | –0.0168 | 6.383 |
| 3950 | 18.189(2) | 0.9997(1) | 0.0003(1) | 0.5569(8) | 2.407(2) | 4.5851 | 5.820 | 0.0533 | 6.388 |
| **$P_{imp}$ = 29.9 GPa** | | | | | | | | | |
| 6700 | 30.023(2) | 0.9930(1) | 0.0070(1) | 0.5001(8) | 3.963(1) | 8.5267 | 10.502 | –0.1103 | 7.890 |
| 6725 | 30.015(2) | 0.9939(1) | 0.0061(1) | 0.5017(8) | 3.960(2) | 8.5392 | 10.503 | –0.0810 | 7.897 |
| 6750 | 30.008(3) | 0.9936(1) | 0.0064(1) | 0.5024(7) | 3.966(3) | 8.5808 | 10.543 | –0.0274 | 7.900 |
| 6775 | 30.009(2) | 0.9926(1) | 0.0075(1) | 0.5008(7) | 3.954(2) | 8.6431 | 10.586 | –0.0089 | 7.892 |
| 6800 | 30.022(2) | 0.9923(1) | 0.0077(1) | 0.5010(7) | 3.957(1) | 8.6847 | 10.624 | 0.0271 | 7.895 |
| **$P_{imp}$ = 36.0 GPa** | | | | | | | | | |
| 7900 | 36.083(3) | 0.9762(1) | 0.0238(1) | 0.4762(9) | 4.666(2) | 10.8830 | 13.204 | –0.1105 | 8.514 |
| 7950 | 36.121(3) | 0.9753(1) | 0.0247(1) | 0.4765(6) | 4.672(2) | 10.9868 | 13.299 | –0.0252 | 8.520 |
| 7975 | 36.100(2) | 0.9750(1) | 0.0250(1) | 0.4766(5) | 4.668(2) | 11.0363 | 13.338 | 0.0233 | 8.518 |
| 8000 | 36.143(2) | 0.9744(1) | 0.0256(1) | 0.4766(5) | 4.677(2) | 11.0924 | 13.395 | 0.0644 | 8.523 |
| 8050 | 36.141(2) | 0.9734(1) | 0.0266(1) | 0.4768(7) | 4.675(2) | 11.2008 | 13.486 | 0.1606 | 8.524 |
| 8475 | 36.120(3) | 0.9648(1) | 0.0352(1) | 0.4796(11) | 4.686(2) | 12.1361 | 14.307 | 1.0393 | 8.537 |
| 8500 | 36.115(3) | 0.9643(1) | 0.0357(1) | 0.4796(5) | 4.682(2) | 12.1932 | 14.352 | 1.0863 | 8.536 |
| 8550 | 36.119(3) | 0.9632(1) | 0.0368(1) | 0.4800(8) | 4.687(2) | 12.3059 | 14.455 | 1.1950 | 8.539 |

Table 3. Constant-pressure RxMC simulations of shocked liquid $N_2$ (continued).

| T (K) | <*P*> (GPa) | Mole Fraction[a] <x($N_2$)> | Mole Fraction[a] < x(N)> | <*V*> ($cm^3$/g) | <$U^{conf}$> (kJ/g) | $H^{ob}$ (kJ/g) | $E^c$ (kJ/g) | $H_g$[d] (kJ/g) | $D^e$ (km/s) |
|---|---|---|---|---|---|---|---|---|---|
| **$P_{imp}$ = 47.0 GPa** | | | | | | | | | |
| 9350 | 47.152(5) | 0.9260(1) | 0.0741(1) | 0.4351(8) | 5.809(3) | 14.9046 | 17.939 | –0.5608 | 9.481 |
| 9450 | 47.182(2) | 0.9221(2) | 0.0779(2) | 0.4352(6) | 5.812(2) | 15.2050 | 18.212 | –0.2958 | 9.485 |
| 9550 | 47.148(2) | 0.9183(2) | 0.0816(2) | 0.4355(3) | 5.805(2) | 15.5024 | 18.473 | –0.0142 | 9.484 |
| 9575 | 47.130(2) | 0.9179(1) | 0.0821(1) | 0.4355(3) | 5.799(2) | 15.5580 | 18.515 | 0.0353 | 9.482 |
| 9600 | 47.134(3) | 0.9166(2) | 0.0834(2) | 0.4357(6) | 5.804(2) | 15.6475 | 18.602 | 0.1249 | 9.483 |
| **$P_{imp}$ = 52.6 GPa** | | | | | | | | | |
| 9500 | 52.740(4) | 0.9101(2) | 0.0899(2) | 0.4160(6) | 6.336(3) | 15.7319 | 19.248 | –1.9974 | 9.911 |
| 9750 | 52.737(3) | 0.9002(2) | 0.0998(2) | 0.4162(4) | 6.325(2) | 16.5027 | 19.934 | –1.3053 | 9.912 |
| 10000 | 52.754(3) | 0.8888(2) | 0.1112(2) | 0.4162(4) | 6.314(3) | 17.3362 | 20.683 | –0.5620 | 9.914 |
| 10250 | 52.755(6) | 0.8774(2) | 0.1226(2) | 0.4164(8) | 6.304(4) | 18.1791 | 21.441 | 0.2006 | 9.915 |
| **$P_{imp}$ = 60.4 GPa** | | | | | | | | | |
| 10400 | 60.527(3) | 0.8498(3) | 0.1502(3) | 0.3925(5) | 6.989(2) | 19.4771 | 23.379 | –1.7771 | 10.469 |
| 10500 | 60.521(4) | 0.8441(2) | 0.1559(2) | 0.3924(5) | 6.979(2) | 19.8615 | 23.724 | –1.4344 | 10.468 |
| 10600 | 60.563(7) | 0.8388(3) | 0.1612(3) | 0.3920(8) | 6.969(4) | 20.2337 | 24.057 | –1.1294 | 10.469 |
| 10900 | 60.551(4) | 0.8231(2) | 0.1769(2) | 0.3916(7) | 6.939(2) | 21.3514 | 25.056 | –0.1370 | 10.466 |
| 10950 | 60.506(3) | 0.8201(3) | 0.1799(3) | 0.3916(6) | 6.928(4) | 21.5531 | 25.231 | 0.0583 | 10.462 |
| 11000 | 60.544(4) | 0.8170(4) | 0.1830(4) | 0.3915(8) | 6.929(2) | 21.7593 | 25.424 | 0.2306 | 10.465 |
| **$P_{imp}$ = 81.1 GPa** | | | | | | | | | |
| 12400 | 81.093(5) | 0.6487(4) | 0.3513(4) | 0.3352(5) | 8.275(4) | 30.8436 | 35.438 | –0.7344 | 11.728 |
| 12500 | 81.075(7) | 0.6416(5) | 0.3584(5) | 0.3347(7) | 8.253(3) | 31.3115 | 35.854 | –0.3281 | 11.724 |
| 12600 | 81.120(8) | 0.6351(4) | 0.3649(4) | 0.3343(8) | 8.240(4) | 31.7590 | 36.259 | 0.0387 | 11.724 |
| **$P_{imp}$ = 91.5 GPa** | | | | | | | | | |
| 13000 | 91.191(9) | 0.5584(6) | 0.4416(6) | 0.3109(7) | 8.775(5) | 35.5438 | 40.461 | –1.3754 | 12.274 |
| 13250 | 91.118(9) | 0.5424(5) | 0.4576(5) | 0.3101(8) | 8.725(4) | 36.6715 | 41.464 | –0.3756 | 12.263 |
| 13500 | 91.092(11) | 0.5267(7) | 0.4733(7) | 0.3092(8) | 8.671(6) | 37.7904 | 42.454 | 0.5857 | 12.255 |
| 15500 | 90.482(12) | 0.4170(6) | 0.5830(6) | 0.3045(11) | 8.242(3) | 46.2912 | 49.933 | 8.1337 | 12.183 |
| 16000 | 90.418(14) | 0.3917(6) | 0.6083(6) | 0.3036(12) | 8.147(4) | 48.3805 | 51.779 | 9.9691 | 12.173 |
| 16500 | 90.064(18) | 0.3599(8) | 0.6401(8) | 0.3022(17) | 7.991(4) | 50.7644 | 53.858 | 12.1530 | 12.141 |

Notes: '< >' indicates ensemble averages determined from the simulation.

Uncertainty in units of the last decimal digit is given in parentheses: 3.010(2) means 3.010 ± 0.002.

[a]Mole fraction of $N_2$, so $x(N_2) = N_{N2}/N_{total}$ and $x(N) = ½\ N_N/N_{total}$, where N total = 3375.

[b]From equation 11.

[c]From equation 14.

[d]From equation 8.

[e]From equation 7.

experimental data is given in table 4. In table 4, the uncertainties for the shock Hugoniot properties measured by experiment are given in parentheses, while the uncertainties in the RxMC calculations can be estimated from the R-square value of the functional fit of data given in table 3. Typical R-square values for the predicted temperatures and specific volumes are 0.97–0.99. Plots of the shock Hugoniot pressure vs. the specific volume and the shock wave velocity are given in figures 1 and 2, respectively, for both the reactive and nonreactive models.

Table 4. Shock Hugoniot states of liquid nitrogen.[a] RxMC results are for the reactive model discussed in the text. Experimental data is taken from Nellis et al. (*55*), except for those noted.

| ***P*** **(GPa)** | | ***V*** **($cm^3$/mol $N_2$)** | | ***T*** **(K)** | | ***D*** **(km/s)** | |
|---|---|---|---|---|---|---|---|
| **Exp.** | **RxMC[b]** | **Exp.** | **RxMC** | **Exp.** | **RxMC** | **Exp.** | **RxMC** |
| 2.96[c] | 2.96 | 21.7 | 21.36 | — | 536.2 | 3.14 | 3.087 |
| 4.74[c] | 4.74 | 20.1 | 19.82 | — | 883.9 | 3.74 | 3.703 |
| 10.1[c] | 10.0 | 17.3 | 17.41 | — | 2008.4 | 5.00 | 4.993 |
| 18.1(0.5) | 18.1 | 15.34(0.5) | 15.57 | 4300(200) | 3912.4 | 6.34 | 6.384 |
| 29.9(0.5) | 29.9 | 14.26(0.5) | 14.05 | 7300(250) | 6778.1 | 7.93 | 7.895 |
| 36.0(0.4) | 36.0 | 13.41(0.4) | 13.35 | 8750(300) | 7963.0 | 8.52 | 8.519 |
| 47.0(0.5) | 47.0 | 11.83(0.5) | 12.20 | 8900(600) | 9557.7 | 9.40 | 9.483 |
| 52.6(0.5) | 52.6 | 11.13(0.5) | 11.66 | 11100(800) | 10185.4 | 9.79 | 9.914 |
| 60.4(0.7) | 60.4 | 10.31(0.7) | 10.97 | 12000(850) | 10935.2 | 10.31 | 10.465 |
| 81.1(1.5) | 81.1 | 9.40(1.5) | 9.366 | 14500(1000) | 12588.9 | 11.73 | 11.724 |

[a]Uncertainties in experimental data (where available) are given in parentheses.
[b]Pressure imposed in the constant-pressure version of the RxMC method.
[c]Taken from Zubarev and Telegin (*54*).

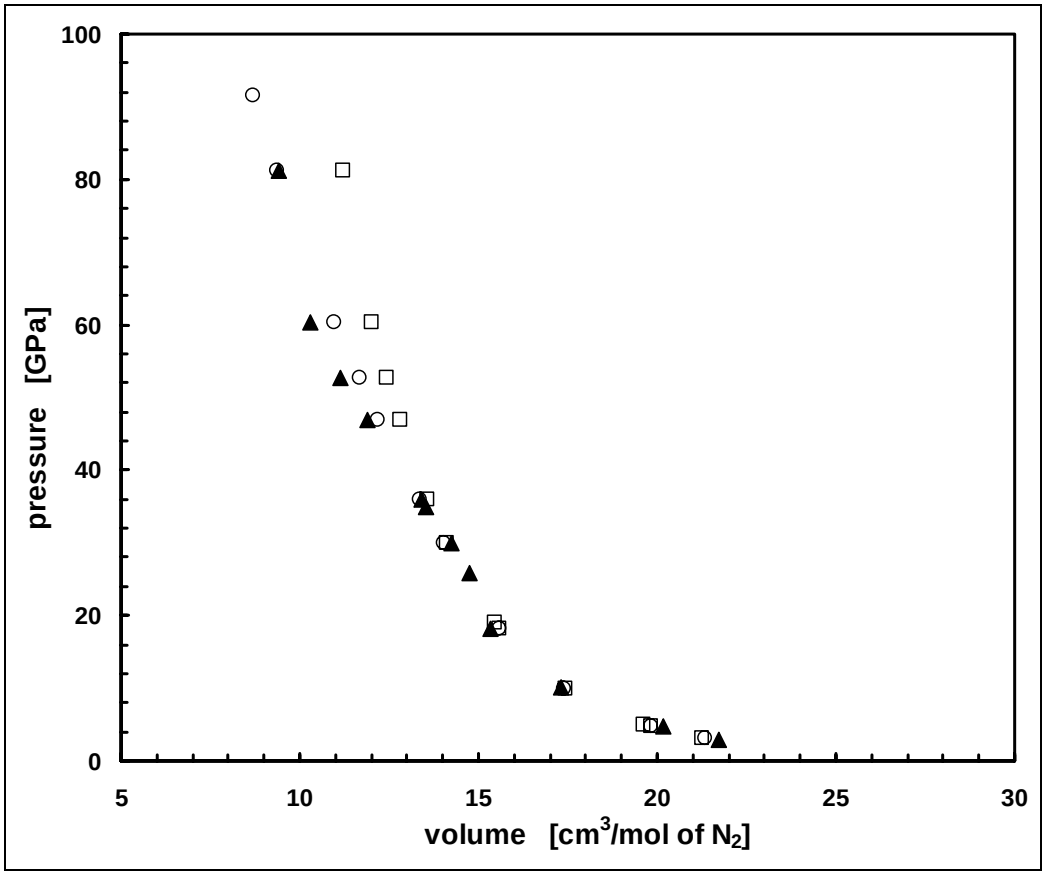


Figure 1. Shock Hugoniot of liquid $N_2$. Calculated values from RxMC simulations using a reactive (○) and nonreactive (□) model are compared with experimental data (▲) (*54*, *55*). The shock pressure is plotted vs. the molar volume of $N_2$.

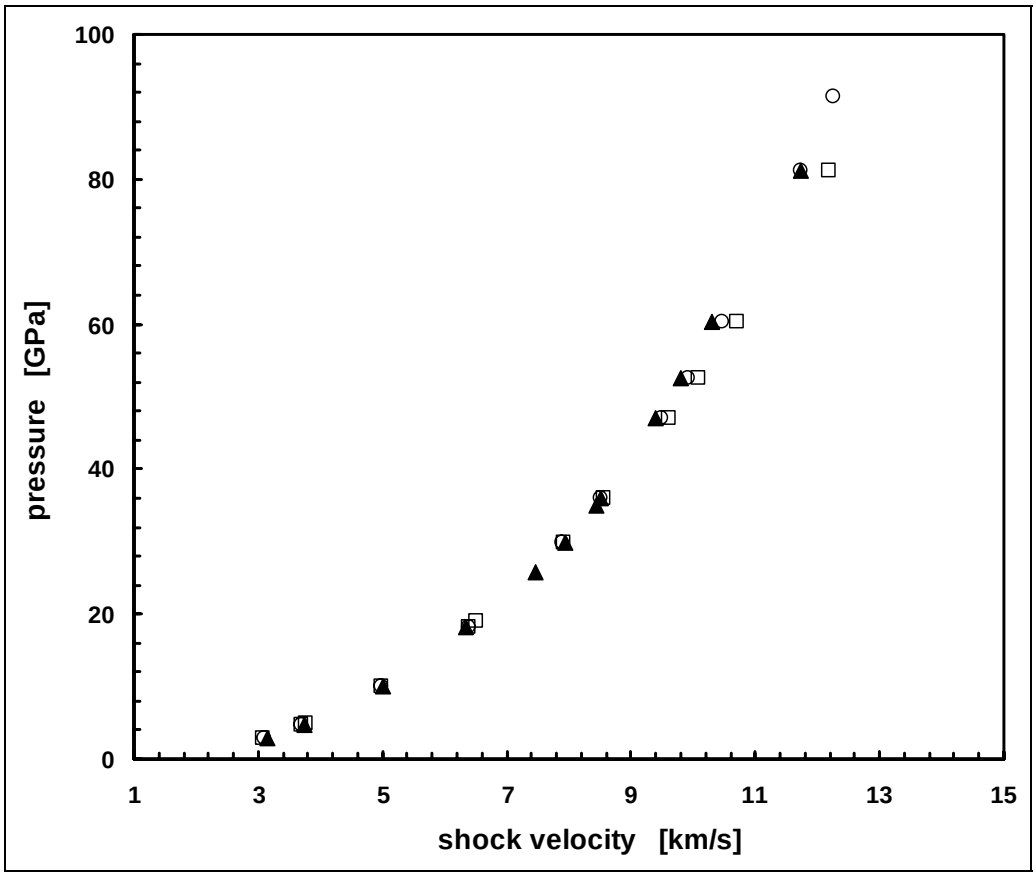


Figure 2. Shock Hugoniot of liquid $N_2$. Calculated values from RxMC simulations (reactive model: [○]; nonreactive model [□]) are compared with experimental data (▲) (*54*, *55*). The shock pressure is plotted vs. the shock wave velocity.

We found excellent agreement between the RxMC calculations using the reactive model and the experimental measurements for most of the pressures considered. As the pressure is increased along the Hugoniot, the system becomes a partially dissociated fluid containing a mixture of $N_2$ molecules and N atoms. This behavior is reflected in the species mole fractions plot of figure 3. Values of the mole fractions shown in figure 3 were determined by interpolating the data reported in table 3 to $T_{Hg}$ using a quadratic function. It is evident from figure 1 that the nonreactive model fails at high pressures where the dissociation is not negligible (*11*).

The experimental data appears to exhibit a softening of the Hugoniot curve near 55 GPa while the RxMC simulations do not predict this behavior. Experimental errors are increasing in this region; therefore, whether the discrepancy is due to experimental uncertainty or an inaccurate model cannot be conclusively established (*11*). Interestingly, however, recent density-functional theory (DFT) calculations (*31*) predict the softening behavior. Pair correlation calculations in the work of Kress et al. (*31*) indicate that the system contains a small fraction of clusters larger than dimers in the partially dissociated region; however, these larger clusters are not long-lived. The dissociated system may contain $N_n$ molecules bound by single (N–N) or single and double

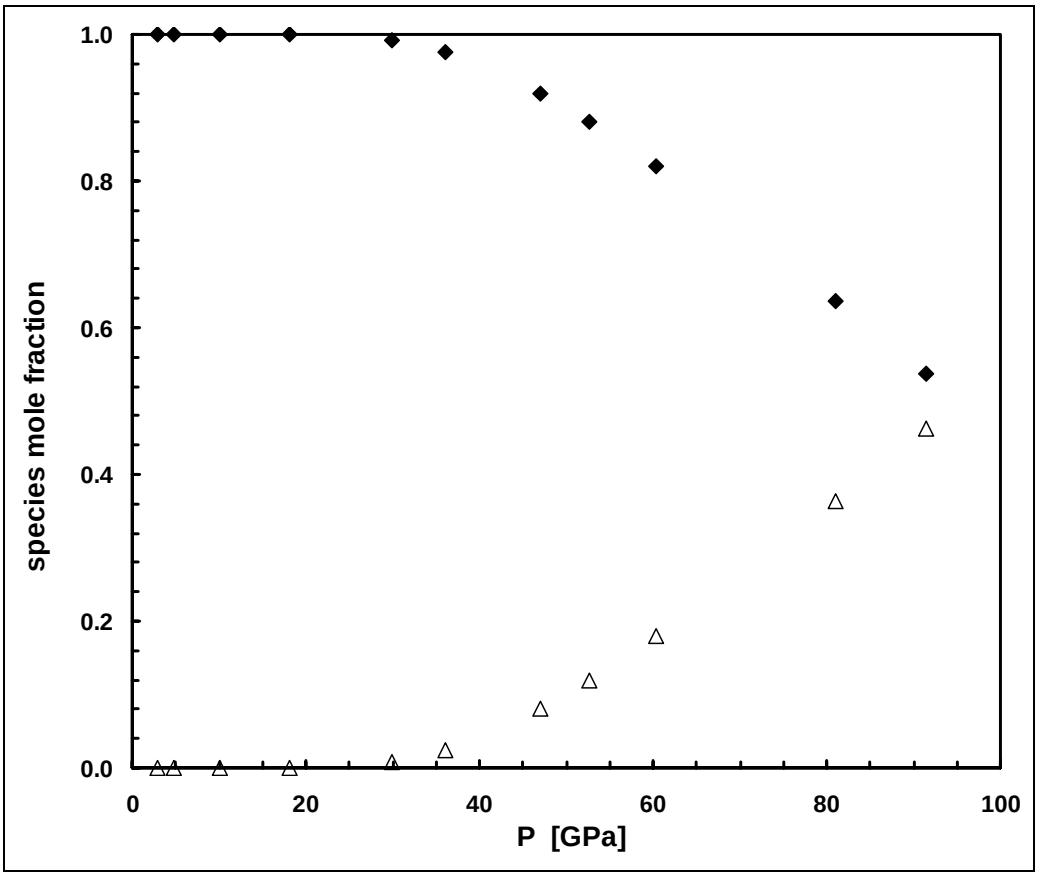


Figure 3. Species mole fractions ($N_2$: [♦]; N: [Δ]) along the Hugoniot curve determined from RxMC simulations of the $N_2$ dissociation reaction.

N ═ N) bonds. Although refining the $N_2$ model is outside the scope of the present work, such products and their accompanying reactions could be included into the RxMC simulation scenario, e.g., N ≡ N⇔N ═ N or N ≡ N⇔N–N, which may make RxMC calculations more compatible with the experimental measurements.

As a matter of curiosity, a point along the Hugoniot curve at $P$ = 91.5 GPa was calculated. Although experimental data are not presently available at this pressure, the recent DFT calculations of Kress and coworkers (*31*) predict considerably different behavior in this pressure regime. The model used in the present work predicts softening behavior ($v$ = 8.68 $cm^3$/mole $N_2$), as does the work of Fried and Howard (*11*), while the DFT calculations appear to be approaching a maximum compression in this region ($v$ = 9.34 $cm^3$/mole $N_2$ at $P$ = 91.5 GPa [*31*]). According to our calculations, such a system would contain a nearly equimolar mixture of $N_2$ molecules and dissociated N atoms (see figure 3).

## 5. Discussion

We have demonstrated the effectiveness of using the RxMC simulation method for determining the shock properties of materials. We found the RxMC calculations to be in excellent agreement with the available experimental data for the $N_2$ dissociation reaction. These results illustrate the utility of the method for predicting the shock Hugoniot for mixtures in which species concentrations are not known and in the absence of interaction potentials that simulate bond breakage and formation. In the next report of this series, we consider an application of the RxMC method to the nitric oxide decomposition reaction ($2NO \Leftrightarrow N_2+O_2$). Several possible extensions of the RxMC are also discussed in the subsequent report (*34*).

## 6. References


1. Touret, J.; van den Kerkhof, A. M. High Density Fluids in the Lower Crust and Upper Mantle. *Physica B & C* **1986**, *139*, 834.

2. Kortbeek, P. J.; Seldam, C. A. T.; Schouten, J. A. Calculation of Thermodynamic Properties of Dense Fluid Neon Using Statistical-Mechanical Perturbation-Theory 2 Results up to GPa and Equations of State. *Mol. Phys.* **1990**, *69*, 1001.

3. Duan, Z.; Moller, N.; Weare, J. H. A General Equation of State for Supercritical Fluid Mixtures and Molecular Dynamics Simulation of Mixture PVTX Properties. *Geochim. Cosmochim. Acta* **1996**, *60*, 1209.

4. Fickett, W.; Davis, W. C. *Detonation*; University of California Press: Berkeley, CA, 1979.

5. Ree, F. H. Supercritical Fluid Phase Separations: Implications for Detonation Properties of Condensed Explosives. *J. Chem. Phys.* **1986**, *84*, 5845.

6. Fried, L. E.; Howard, W. M. The Equation of State of Supercritical HF, HCI, and Reactive Supercritical Mixtures Containing the Elements H, C, F, and CT. *J. Chem. Phys.* **1999**, *110*, 12023.

7. Ree, F. H.; Viecelli, J. A.; van Thiel, M. Influence of Fluorine Chemistry on Supercritical Fluid-Fluid Phase Separations. *J. Mol. Liq.* **2000**, *85*, 229.

8. Ross, M. A High-Density Fluid-Perturbation Theory Based on an Inverse 12th-Power Hard-Sphere Reference System. *J. Chem. Phys.* **1979**, *71*, 1567.

9. Zerah, G.; Hansen, J. Self-Consistent Integral Equation for Fluid Pair Distribution Functions: Another Attempt. *J. Chem. Phys.* **1986**, *84*, 2336.

10. Vortler, H. L.; Nezbeda, I.; Lísal, M. The Exp-6 Potential Fluid at Very High Pressures: Computer Simulations and Theory. *Mol. Phys.* **1997**, *92*, 813.

11. Fried, L. E.; Howard, W. M. An Accurate Equation of State for the Exponential-6 Fluid Applied to Dense Supercritical Nitrogen. *J. Chem. Phys.* **1998**, *109*, 7338.

12. Ree, F. H. A Statistical Mechanical Theory of Chemically Reacting Multiphase Mixtures: Application to the Detonation Properties of PETN. *J. Chem. Phys.* **1984**, *81*, 1251.

13. Fried, L. E. *Cheetah 3.0 User's Manual*; Lawrence Livermore National Laboratory: Livermore, CA, Revision 3, 2001.

14. Karo, A. M.; Hardy, J. R.; Walker, F. E. Theoretical Studies of Shock-Initiated Detonations. *Acta Astronaut* **1978**, *5*, 1041.

15. Batteh, J. H.; Powell, J. D. Shock Propagation in One-Dimensional Lattice at a Non-Zero Initial Temperature. *J. Appl. Phys*. **1978**, *49*, 3933.

16. Batteh, J. H.; Powell, J. D. Solitary-Wave Propagation in the 3-Dimensional Lattice. *Phys. Rev. B* **1979**, *20*, 1398.

17. Powell, J. D.; Batteh, J. H. Effects of Solitary Waves Upon the Shock Profile in a 3-Dimensional Lattice. *J. Appl. Phys.* **1980**, *51*, 2050.

18. Holihan, B. L.; Hoover, W. G.; Moran, B.; Straub, G. K. Shock-Wave Structure via Nonequilibrium Molecular Dynamics and Navier-Stokes Continuum Mechanics. *Phys. Rev. A* **1980**, *22*, 2798.

19. Tsai, D. H.; Trevino, S. F. Simulation of the Initiation of Detonation in an Energetic Molecular Crystal. *J. Chem. Phys.* **1984**, *81*, 5636.

20. Tsai, D. H. *Chemistry and Physics of Energetic Materials*; Bulusu, S. N., Ed.; Kluwer: Dordrecht, 1990.

21. Brenner, D. W. Molecular Potentials for Simulating Shock-Induced Chemistry. In *Shock Compression of Condensed Matter*; Elsevier: Amsterdam, 1992.

22. Robertson, D. H.; Brenner, D. W.; Elert, M. L.; White, C. T. Simulations of Chemically Sustained Shock Fronts in a Model Energetic Material. In *Shock Compression of Condensed Matter;* Elsevier: Amsterdam, 1992.

23. White, C. T.; Robertson, D. H.; Elert, M. L.; Brenner, D. W. Molecular Dynamics Simulations of Shock-Induced Chemistry: Application to Chemically Sustained Shock Waves. In *Microscopic Simulations of Complex Hydrodynamic Phenomena*; Plenum: New York, 1992.

24. Erpenbeck, J. J. Molecular Dynamics of Detonation I. Equation of State and Hugoniot Curve for a Simple Reactive Fluid. *Phys. Rev. A* **1992**, *46*, 6406.

25. Brenner, D. W.; Robertson, D. H.; Elert, M. L.; White, C. T. Detonations at Nanometer Resolution Using Molecular Dynamics. *Phys. Rev. Lett.* **1993**, *70*, 2174.

26. White, C. T.; Sinnott, S. B.; Mintmire, J. W.; Brenner D. W.; Robertson, D. H. Chemistry and Phase Transitions From Hypervelocity Impacts. *Int. J. Quantum Chem. Symp.* **1994**, *28*, 129.

27. Rice, B. M.; Mattson, W.; Grosh, J.; Trevino, S. F. Molecular Dynamics Study of Detonation I. A Comparison With Hydrodynamic Predictions. *Phys. Rev. E* **1996**, *53*, 611.

28. Rice, B. M.; Mattson, W.; Grosh, J.; Trevino, S. F. Molecular Dynamics Study of Detonation II. The Reaction Mechanism. *Phys. Rev. E* **1996**, *53*, 623.

29. Maillet, J. B.; Mareschal, M.; Soulard, L.; Ravelo, R.; Lomdahl, P. S.; Germann, T. C.; Holian, B. L. Uniaxial Hugoniostat: A Method for Atomistic Simulations of Shocked Materials. *Phys. Rev. E* **2000**, *63*, 016121.

30. Swanson, D. R.; Mintmire, J. W.; Robertson, D. H.; White, C. T. Detonation Hugoniots from Molecular Dynamics Simulations. *Chem. Phys. Reps.* **2000**, *18*, 1871.

31. Kress, J. D.; Mazevet, S.; Collins, L. A.; Wood, W. W. Density-Functional Calculation of the Hugoniot of Shocked Nitrogen. *Phys. Rev. B.* **2000**, *63*, 024203.

32. Johnson, J. K.; Panagiotopoulos, A. Z.; Gubbins, K. E. Reactive Canonical Monte Carlo - A New Simulation Technique for Reacting or Associating Fluids. *Mol. Phys.* **1994**, *81*, 717.

33. Smith, W. R.; Tříska, B. J. The Reaction Ensemble Method for the Computer Simulation of Chemical and Phase Equilibria. I. Theory and Basic Examples. *Chem. Phys.* **1994**, *100*, 3019.

34. Brennan, J. K.; Rice, B. M. Molecular Dynamics Simulations of $SiO_2$. U.S. Army Research Laboratory: Aberdeen Proving Ground, MD, submitted for publication, 2005.

35. Reed, T. M.; Gubbins, K. E. *Applied Statistical Mechanics*; McGraw-Hill: New York, NY, 1973.

36. McQuarrie, D. A. *Statistical Mechanics*; Harper: New York, NY, 1976.

37. Chase, M. W.; Davies, C. A.; Downey, J. R.; Frurip, D. J.; McDonald, R. A.; Syverud, A. N. *JANAF Thermochemical Tables*, Third Edition, *J. Phys. Chem.* Ref. Data **1985**, *14*.

38. Johnson, J. K. Reactive Canonical Monte Carlo. *Adv. Chem. Phys.* **1999**, *105*, 461.

39. Lísal, M.; Smith, W. R. Institute of Chemical Process Fundamentals, Academy of Sciences of the Czech Republic. Private communication, 2002.

40. Lísal, M.; Nezbeda, I.; Smith, W. R. The Reaction Ensemble Method for the Computer Simulation of Chemical and Phase Equilibria. II. The $Br_2 + Cl_2 +$ BrCL System. *J. Chem. Phys.* **1999**, *110*, 8597.

41. Lísal, M.; Smith, W. R.; Nezbeda, I. Accurate Computer Simulation of Phase Equilibrium for Complex Fluid Mixtures. Application to Binaries Involving Isobutene, Methanol, Methyl Tert-Butyl Ether, and N-Butane. *J. Phys. Chem. B* **1999**, *103*, 10496.

42. Lísal, M.; Smith, W. R.; Nezbeda, I. Computer Simulation of the Thermodynamic Properties of High-Temperature Chemically-Reacting Plasmas. *J. Chem. Phys.* **2000**, *113*, 4885.

43. Turner, C. H.; Johnson, J. K.; Gubbins, K. E. Effects of Confinement on Chemical Reaction Equilibria: The Reaction $2NO \Leftrightarrow (NO)_2$ and $N_2 + 3H_2 \Leftrightarrow 2NH_3$ in Carbon Micropores. *J. Chem. Phys.* **2001**, *114*, 1851.

44. Borówko, M.; Zagórski, R. Chemical Equilibria in Slit-Like Pores. *J. Chem. Phys.* **2001**, *114*, 5397.

45. Turner, C. H.; Brennan, J. K.; Johnson, J. K.; Gubbins, K. E. Effects of Confinement by Porous Materials on Chemical Reaction Kenetics. *J. Chem. Phys.* **2002**, *116*, 2138.

46. Turner, C. H.; Brennan, J. K.; Pikunic, J. P.; Gubbins, K. E. Simulation of Chemical Reaction Equilibria and Kinetics in Heterogeneous Carbon Micropores. *App. Surf. Sci.*, in press, 2002.

47. Metropolis, N.; Rosenbluth, A. W.; Rosenbluth, M. N.; Teller, A. E.; Teller, E. Equation of State Calculations by Fast Computing Machines. *J. Chem. Phys.* **1953**, *21*, 1087.

48. Lofthus, A.; Krupenie, P. H. *J. Phys. Chem.* Ref. Data, **1977**, *6*, 113.

49. Moore, C. E.; Gallagher, J. W. *Tables of Spectra of Hydrogen, Carbon, Oxygen Atoms and Ions, CRC Series in Evaluated Data in Atomic Physics*; Chemical Rubber: Boca Raton, FL, 1993.

50. Curtiss, L. A.; Redfern, P. C.; Furip, D. J. *Reviews in Computational Chemistry*; Lipkowitz K. B., Boyd, D. B., Eds.; Wiley-VCH, John Wiley and Sons, Inc.: New York, NY, 2000; Vol. 15, pp 147.

51. Ochterski, J. W. Thermochemistry in Gaussian. http://www.gaussian.com (accessed 2000), Gaussian, Inc.

52. Frenkel, D.; Smit, B. *Understanding Molecular Simulation*; Academic Press: San Diego, CA, 1996.

53. Allen, M. P.; Tildesley, D. J. *Computer Simulation of Liquids*; Oxford University Press: Oxford, UK, 1987.

54. Zubarev, V. N.; Telegin, G. S. Calculation of Parameters of Detonation Waves From Condensed Explosives. *Sov. Phys. Dokl*. **1962**, *7*, 34.

55. Nellis, W. J.; Radousky, H. B.; Hamilton, D. C.; Mitchell, A. C.; Holmes, N. C.; Christianson, K. B.; van Thiel, M. Equation-of-State, Shock-Temperature, and Electrical-Conductivity Data of Dense Fluid Nitrogen in the Region of the Dissociative Phase Transition. *J. Chem. Phys.* **1991**, *94*, 2244.

56. Radousky, H. B.; Nellis, W. J.; Ross, M.; Hamilton, D. C.; Mitchell, A. C. Molecular Dissociation and Shock-Induced Cooling in Fluid Nitrogen at High Densities and Temperatures. *Phys. Rev. Lett.* **1986**, *57*, 2419.

57. Ross, M. The Dissociation of Dense Liquid Nitrogen. *J. Chem. Phys.* **1987**, *86*, 7110.

58. McMahan, A. K.; LeSar, R. Pressure Dissociation of Solid Nitrogen Under 1 Mbar. *Phys. Rev. Lett.* **1985**, *54*, 1929.

59. Martin, R. M.; Needs, R. J. Revision B, **1986**, *34*, 5082.

60. van Thiel, M.; Ree, F. H. Accurate High-Pressure and High-Temperature Effective Pair Potentials for the Systems $N_2$–N and $O_2$–O. *J. Chem. Phys.* **1986**, *104*, 5019.

61. Hamilton, D. C.; Ree, F. H. Chemical Equilibrium Calculations on the Molecular-to-Nonmolecular Transition of Shock Compressed Liquid Nitrogen. *J. Chem. Phys.* **1989**, *90*, 4972.

62. Ross, M. Shock Compression of Simple Liquids: Implications for Deuterium. *High Press. Res.* **2000**, *16*, 371.

NO. OF
COPIES ORGANIZATION

1 (PDF ONLY) DEFENSE TECHNICAL INFORMATION CTR
DTIC OCA
8725 JOHN J KINGMAN RD
STE 0944
FORT BELVOIR VA 22060-6218

1 US ARMY RSRCH DEV & ENGRG CMD
SYSTEMS OF SYSTEMS INTEGRATION
AMSRD SS T
6000 6TH ST STE 100
FORT BELVOIR VA 22060-5608

1 DIRECTOR
US ARMY RESEARCH LAB
IMNE ALC IMS
2800 POWDER MILL RD
ADELPHI MD 20783-1197

3 DIRECTOR
US ARMY RESEARCH LAB
AMSRD ARL CI OK TL
2800 POWDER MILL RD
ADELPHI MD 20783-1197

ABERDEEN PROVING GROUND

1 DIR USARL
AMSRD ARL CI OK TP (BLDG 4600)

NO. OF
COPIES ORGANIZATION

1 DIRECTOR
US ARMY RESEARCH LAB
AMSRD ARL D
J MILLER
2800 POWDER MILL RD
ADELPHI MD 20783-1197

2 DIRECTOR
US ARMY RESEARCH LAB
AMSRD ARL RO P
R SHAW
TECH LIB
PO BOX 12211
RESEARCH TRIANGLE PARK NC
27709-2211

1 CDR US ARMY ARDEC
TECH LIB
PICATINNY ARSENAL NJ 07806-5000

1 CDR NAVAL RSRCH LAB
TECH LIBRARY
WASHINGTON DC 20375-5000

1 OFFICE OF NAVAL RSRCH
J GOLDWASSER
875 N RANDOLPH ST RM 653
ARLINGTON VA 22203-1768

1 CDR
NAVAL SURFACE WARFARE CTR
TECH LIB
INDIAN HEAD MD 20640-5000

1 CDR
NAVAL SURFACE WARFARE CTR
TECH LIB
DAHLGREN VA 22448-5000

1 AIR FORCE RSRCH LAB
MNME EN MAT BR
B WILSON
2306 PERIMETER RD
EGLIN AFB FL 32542-5910

1 AIR FORCE OFC OF SCI RSRCH
M BERMAN
875 N RANDOLPH ST
STE 235 RM 3112
ARLINGTON VA 22203-1768

NO. OF
COPIES ORGANIZATION

1 DIR SANDIA NATL LABS
M BAER DEPT 1512
PO BOX 5800
ALBUQUERQUE NM 87185

1 DIR LAWRENCE LIVERMORE NL
L FRIED
PO BOX 808
LIVERMORE CA 94550-0622

1 UNIV OF ALABAMA
DEPT OF CHEMICAL ENGRG
C TURNER
A132 BEVILL
TUSCALOOSA AL 35487-0286

ABERDEEN PROVING GROUND

61 DIR USARL
AMSRD ARL WM
T ROSENBERGER
AMSRD ARL WM M
S MCKNIGHT
AMSRD ARL WM T
B BURNS
AMSRD ARL WM TB
P BAKER
AMSRD ARL WM BD
R ANDERSON
W ANDERSON
R BEYER
A BRANT
G BROWN
S BUNTE
C CANDLAND
W CIEPIELA
G COOPER
L CHANG
T COFFEE
J COLBURN
P CONROY
B DAVIS
J DESPIRITO
N ELDREDGE
B FORCH
J GARNER
D HEPNER
B HOMAN
A HORST

NO. OF
COPIES ORGANIZATION

S HOWARD
P KASTE
G KATULKA
T KOGLER
A KOTLAR
C LEVERITT
R LIEB
D LYON
K MCNESBY
M MCQUAID
M MILLER
A MIZIOLEK
J MORRIS
J NEWBERRY
J NEWILL
M NUSCA (6 CPS)
W OBERLE
R PESCE-RODRIGUEZ
P PLOSTINS
S PIRIANO
G REEVES
B RICE
J SAHU
R SAUSA
S SILTON
E SCHMIDT
J SCHMIDT
P WEINACHT
D WILKERSON
A WILLIAMS
M ZOLTOSKI

NO. OF
COPIES ORGANIZATION

1 ACADEMY OF SCIENCES
OF THE CZECH REPUBLIC
E HALA LABORATORY
OF THERMODYNAMICS
M LISAL
165 02 PRAGUE 6-SUCHDOL
CZECH REPUBLIC

INTENTIONALLY LEFT BLANK.